Voltage-Dependent Gating of Single Gap Junction Channels in an Insect Cell Line

Feliksas F. Bukauskas and Robert Weingart
Department of Physiology, University of Bern, Bühlplatz 5, CH-3012 Bern, Switzerland

ABSTRACT *De novo* formation of cell pairs was used to examine the gating properties of single gap junction channels. Two separate cells of an insect cell line (clone C6/36, derived from the mosquito *Aedes albopictus*) were pushed against each other to provoke formation of gap junction channels. A dual voltage-clamp method was used to control the voltage gradient between the cells (V_j) and measure the intercellular current (I_j). The first sign of channel activity was apparent 4.7 min after cell contact. Steady-state coupling reached after 30 min revealed a conductance of 8.7 nS. Channel formation involved no leak between the intra- and extracellular space. The first opening of a newly formed channel was slow (25–28 ms). Each preparation passed through a phase with only one operational gap junction channel. This period was exploited to examine the single channel properties. We found that single channels exhibit several conductance states with different conductances γ_j: a fully open state (γ_j(*main state*)), several substates (γ_j(*substates*)), a residual state (γ_j(*residual*)) and a closed state (γ_j(*closed*)). The γ_j(*main state*) was 375 pS, and γ_j(*residual*) ranged from 30 to 90 pS. The transitions between adjacent substates were 1/7–1/4 of γ_j(*main state*). V_j had no effect on γ_j(*main state*), but slightly affected γ_j(*residual*). The I_j transitions involving γ_j(*closed*) were slow (15–60 ms), whereas those not involving γ_j(*closed*) were fast (< 2 ms). An increase in V_j led to a decrease in open channel probability. Depolarization of the membrane potential (V_m) increased the incidence of slow transitions leading to γ_j(*closed*). We conclude that insect gap junctions possess two gates, a fast gate controlled by V_j and giving rise to γ_j(*substates*) and γ_j(*residual*), and a slow gate sensitive to V_m and able to close the channel completely.

INTRODUCTION

Over the last decade, cell pairs have been used extensively to study the properties of gap junctions. The preparations were obtained from incomplete dissociation of tissues, or after *de novo* formation in cell cultures. Particularly productive cell pair experiments were performed in conjunction with the dual voltage-clamp method. As a result, our knowledge of biophysical and biochemical functions of gap junctions expanded quickly (e.g., Bennett and Verselis, 1992). It is generally recognized that gap junctions from various sources differ in their properties, e.g., the sensitivity to voltage, second messengers, Ca^{2+}, H^+, or pharmacological agents. Expression studies of cloned connexin DNAs in *Xenopus* oocytes or transfected cells have confirmed that different connexins are responsible for the functional diversity (for review, see Bennett and Verselis, 1992). However, despite their success, cell pair experiments suffer from several limitations. A major problem is that the analysis of single gap junction channels cannot be readily accomplished in cell pairs. Usually, the gap junction of a cell pair consists of many channels in parallel, typically several hundred. Yet, for such studies an ideal preparation contains only one channel. In order to render cell pairs suitable for single-channel analysis, the number of operational channels must be reduced. A widely used experimental approach consists of exposure to submaximal doses of uncoupling agents, such as long-chain alkanols (Burt and Spray, 1988) or arachidonic acid (Giaume et al., 1989). However, these interventions are likely to introduce new problems. For example, the uncoupling agents may affect the parameters under investigation, e.g., the single channel conductance or the open channel probability. Also, single channel data revealing multiple conductances cannot be interpreted unequivocally in terms of functional models (Chen and DeHaan, 1992).

In order to circumvent these difficulties, we resorted to a different experimental approach. It consists of pushing two single cells together to establish a physical contact between their cell membranes and thereby allow *de novo* formation of gap junction channels. In other contexts, this approach has been used before to examine *Xenopus* blastulae (Loewenstein et al., 1978), embryonic *Xenopus* muscle cells (Chow and Poo, 1984; Chow and Young, 1987), and neonatal rat heart cells (Rook et al., 1988).

The experiments presented in this paper have been performed with an established cell line derived from larvae of the mosquito *Aedes albopictus* (clone C6/36; Igarashi, 1978). Insect cells seemed particularly appropriate for this investigation. Previous studies indicated that their gap junction channels exhibit large conductances (Bukauskas and Weingart, 1993). This helps to improve the signal/noise ratio and hence allows a better resolution of junctional currents. In addition, insect gap junctions possess a versatile set of properties. Their channels exhibit two different voltage-sensitive gates, one controlled by the transjunctional voltage gradient, V_j, and the other by the membrane potential, V_m (Verselis et al., 1991; Bukauskas et al., 1992; Weingart et al., 1993).

In this study, we explored the *de novo* formation of gap junction channels and studied their voltage-dependent

Received for publication 9 December 1993 and in final form 18 May 1994.
Address reprint requests to Robert Weingart, Department of Physiology, Bühlplatz 5, CH-3012 Bern, Switzerland. Tel.: 41 31 631 8711; Fax: 41 31 631 4611.

0006-3495/94/08/613/13 $2.00

properties. Preliminary data have been published before (Bukauskas and Weingart, 1993; Weingart and Bukauskas, 1993).

METHODS

Cells

Cells of an insect cell line (clone C6/36, derived from larvae of the mosquito *Aedes albopictus*; Igarashi, 1978) were grown at 28°C in culture medium (RPMI 1640, GIBCO, Paisley, UK) containing 20% fetal calf serum, 100 μg/ml streptomycin and 100 U/ml penicillin (code 2212, Biochrom, Berlin, Germany). The cells were passaged weekly and diluted 1:10. For the experiments, monolayers of cells ($\sim 4 \cdot 10^5$ cells/cm^2) were harvested and resuspended in RPMI 1640 containing 20% fetal calf serum at a cell density of $0.2–1 \cdot 10^6$ cells/ml. Thereafter, the cells were seeded at a density of $\sim 10^4$ cells/cm^2 onto sterile glass coverslips placed in multiwell culture dishes. Electrophysiological measurements were carried out 1–3 days after plating.

Solutions and pipettes

All experiments were performed in modified Krebs-Ringer solution (mM): NaCl 140, KCl 4, $CaCl_2$ 2, $MgCl_2$ 1, HEPES 5 (pH adjusted to 7.4), glucose 5, pyruvate 2. Patch pipettes were pulled from glass capillaries (GC150TF-10; Clark Electromedical Instruments, Pangbourne, UK) using a horizontal puller (BB-CH, Mécanex, Geneva, Switzerland). Immediately before use, the pipettes were filled with an electrolyte solution of the following composition (mM): NaCl 10, potassium aspartate 120, $CaCl_2$ 1, $MgCl_2$ 1, MgATP 3, HEPES 5 (pH 7.2), EGTA 10 (pCa ~8), filtered through 0.22-μm pores. When filled, the pipettes had direct current resistances of 3–5 MΩ (tip size, ~1 μm).

Electrical measurements

The experimental chamber, consisting of a Perspex frame with a glass bottom, was mounted on the stage of an inverted microscope equipped with phase-contrast optics (Diaphot-TMD, Nikon; Nippon Kogaku, Tokyo, Japan). It was perfused with Krebs-Ringer solution at room temperature (22–26°C) using a gravity system (bath volume, 1 ml; flow rate, 1–2 ml/min). A video system (CCD-camera, Panasonic WV-CD52; monitor: Panasonic WV-5410; Matsushita Electric Industrial, Osaka, Japan) facilitated the optical supervision of the cells and pipettes during an experiment.

To study the electrical properties of gap junction channels, a dual voltage-clamp method was used that has been described in detail (Weingart, 1986). In brief, coverslips with adherent cells were transferred from culture dishes to the experimental chamber. Two single cells in close proximity were selected visually under the microscope. Each cell was then brought into contact with a patch pipette connected to a separate clamp amplifier (EPC 7; List Electronic, Darmstadt, Germany). After establishment of the whole-cell, tight-seal recording conditions, the cells were pushed together by moving the patch pipettes with hydraulic micromanipulators (WR-88, Narishige Scientific Instrument, Tokyo, Japan). This approach allowed us to control the membrane potential of each cell individually (V_1, V_2) and monitor the associated currents through both pipettes separately (I_1, I_2). In the case of two separate cells, I_1 and I_2 reflect the currents through the membranes of cells 1 ($I_{m,1}$) and 2 ($I_{m,2}$), respectively. After establishment of an intercellular communication, I_1 and I_2 represent the sum of two currents, $I_{m,1} + I_j$ (I_j, current through gap junction) and $I_{m,2} - I_j$, respectively. Deflections in I_1 and I_2, coincident in time and opposite in polarity, correspond to changes in gap junctional currents. The conductance of a gap junction channel was determined as $\gamma_j = (V_2 - V_1)/\Delta I_j$.

Signal recording and analysis

Voltage and current signals were recorded on FM tape (SE 3000, SE Lab, Feltham, UK) at 3¾ ips (direct current bandwidth: 2.5 kHz). For offline analysis with a personal computer, the current signals were filtered at 1 kHz (−3 dB) using an 8-pole Bessel filter (902LPF, Frequency Devices, Haverhill, MA, USA) and digitized at 3.33 kHz with a 12-bit A/D converter (IDA 12120; INDEC Systems, Capitola, CA, USA). Data analysis was carried out with an acquisition system (C-Lab, INDEC Systems). Measurements of membrane potentials were corrected for the liquid junction potential between pipette solution and bath solution (−12 mV). The results are presented as mean ± 1 SEM.

The following terminology will be used. "Formation of a gap junction channel" involves two consecutive processes, "docking" (assembly) of two hemichannels (connexons), and "first opening" of the entire gap junction

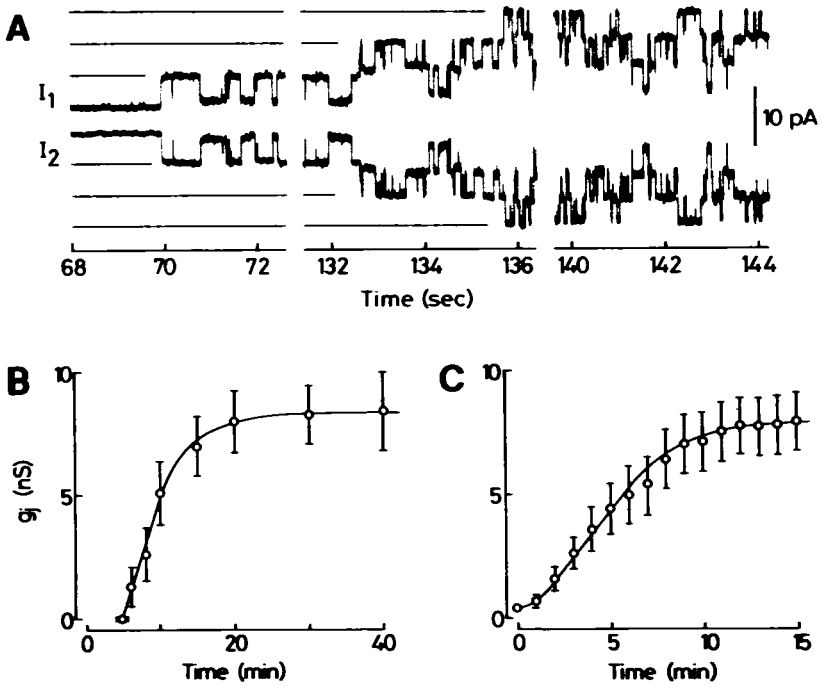

FIGURE 1 Formation of a gap junction between two single cells. (*A*) The membrane potentials of cells 1 and 2 (V_1, V_2, not shown) were clamped to −60 mV and −75 mV, respectively, and the accompanying membrane currents were measured (I_1, I_2). Physical contact between the cells was established at $t = 0$ s. Synchronous transitions in I_1 and I_2, identical in amplitude and of opposite polarity, reflect gap junction events (channel opening is indicated by upward deflections in I_1 and downward deflections in I_2). Note that the records were interrupted after 72 s and 136 s. (*B*) Plot of gap junction conductance, g_j, versus time, emphasizing the lag period in gap junction formation. $t = 0$ min corresponds to the moment of physical contact between the cells. Dots and bars represent means ± 1 S.E.M., respectively, from 32 cell pairs. (*C*) Plot of g_j versus time, emphasizing the process of channel formation. $t = 0$ min corresponds to the event of first channel opening. The data were fitted by the Hill equation, $g_j = g_j(\max) \cdot t^n/(t^n + K^n)$, with the parameters $g_j(\max) = 8.7$ nS, $K = 4.8$, $n = 1.9$.

channel. "Formation of a gap junction" involves sequential opening of new gap junction channels.

RESULTS

Formation of gap junctions

Coverslips with adherent cells were screened visually for two single cells in close proximity. Each cell was then connected to a patch pipette to form a giga-Ω seal. After disruption of the membrane patches, the conditions for whole-cell voltage-clamping were established. To impose a voltage gradient across the presumptive gap junction, the membrane potentials of cells 1 (V_1) and 2 (V_2) were clamped to different levels. Thereafter, the cells were pushed against each other by gently moving the patch pipettes via micromanipulators.

Fig. 1 illustrates the subsequent formation of a gap junction. Fig. 1 *A* shows segments of the continuous current records documenting the consecutive opening of the first three gap junction channels. Physical contact between the cells was established at time $t = 0$ s. Traces I_1 and I_2 represent the currents of cells 1 and 2, respectively, driven by a sustained junctional voltage gradient, $V_j = V_2 - V_1 = -15$ mV ($V_1 = -60$ mV; $V_2 = -75$ mV). Simultaneous transitions in I_1 and I_2, comparable in amplitude and opposite in polarity, indicate the operation of gap junction channels. The first opening of the first channel occurred around $t = 70$ s (upward deflection in I_1; downward deflection in I_2). After this event, the currents exhibited several transitions attributable to closing and reopening of the first channel. The first sign of a second channel was visible around $t = 133$ s. Thereafter, I_1 and I_2 revealed synchronous fluctuations involving three major current levels. The first opening of a third channel was observed around $t = 136$ s. After approximately 10 min, I_1 and I_2 reached a stable level (not shown).

Using this approach, we observed the *de novo* formation of a gap junction in 61 out of 91 preparations. Figs. 1 *B* and 2 *C* show the time course of gap junction formation summarizing the results from those experiments that lasted >30 min ($n = 32$). Values of the gap junction conductance, $g_j = I_j/V_j$, were calculated for each preparation, averaged, and plotted versus time. Early during each experiment (i.e., up until the insertion of 3 to 4 channels), a V_j gradient was maintained continuously; later, a V_j pulse of 200 ms duration was administered to cell 1 every second.

In Fig. 1 *B*, $t = 0$ min corresponds to the moment when the physical contact between the cells was established. Hence, this plot documents the lag period in gap junction formation. After a variable delay, g_j began to increase and eventually reached a steady state. The lag phase between cell contact and first channel activity was 4.7 ± 0.6 min, the steady-state conductance reached at $t = 30$ min was 8.7 ± 1.4 nS. In Fig. 1 *C*, $t = 0$ min corresponds to the time of first channel opening. Hence, the plot emphasizes the process of channel formation. It shows that g_j increased with time in a sigmoid manner, implying that channel formation occurred in a cooperative manner. The data were fitted by a Hill equation with a cooperativity of 1.9.

Kinetics of first channel opening

To study the process of channel formation in more detail, current signals were displayed on an expanded time scale. Fig. 2 *A* shows records which document the first opening of a channel. V_j was set to −15 mV (upper panel), −28 mV (center panel), and −44 mV (lower panel), respectively. The traces reveal that the event of first opening was unusual. For example, the rate of I_j increase was slow; I_j took 15–60 ms to reach a steady level. For comparison, I_j transitions associated with subsequent channel closings and openings were fast (<2 ms). In addition, the contour of I_j changed in a V_j-dependent manner. At small V_j, the increase in I_j was smooth (upper panel); at large V_j it was discontinuous (lower panels) implying the involvement of discrete current levels. The signals shown in Fig. 2 *A* and others were used to examine the relation between the duration of a transition during first channel opening, $T_o(slow)$, and V_j. The analysis revealed that $T_o(slow)$ does not depend on V_j prevailing during channel formation (regression coefficient $r = 0.21$; $2\alpha > 0.1$). On average, $T_o(slow)$ was 28 ± 3 ms ($n = 42$).

The slow and complex kinetics of first openings appears to be a general phenomenon. It was not only observed in conjunction with the formation of the first channel of a preparation, but also with the formation of subsequent channels.

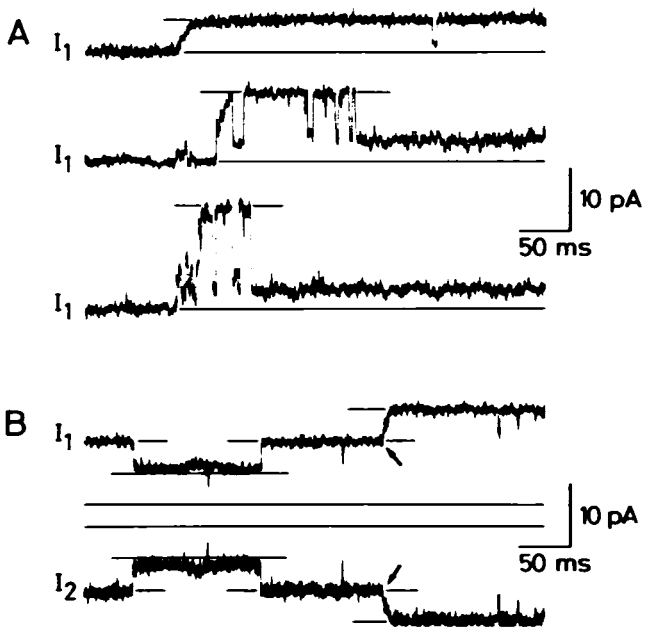

FIGURE 2 First opening of a new gap junction channel. (*A*) Examples of first openings in case of a preparation with one channel. Examples of first channel openings. Selected records of I_1 associated with a transjunctional voltage gradient, V_j, of −15 mV (top), −28 mV (center), and −44 mV (bottom), respectively. Upward (downward) deflections correspond to channel openings (closings). First channel openings were smooth at small V_j and discontinuous at large V_j. In addition, first openings were slow, whereas subsequent closings/openings were fast. The solid lines represent the zero current level or the current level associated with a fully open channel. (*B*) Example of a first opening in case of a preparation with three channels. V_1 was held at −60 mV, V_2 at −75 mV. Initially, the two channels present caused fast transitions in I_1 and I_2 (left side). The first opening of the third channel gave rise to a slow transition in I_1 and I_2 (see *arrows*).

Fig. 2 *B* illustrates an example of first opening in the case of the third channel of a cell pair. In some experiments, before successful first channel opening, I_1 exhibited small transient changes (Fig. 2 *A*, center panel). The transients in I_1 were accompanied by mirror-image transients in I_2 and thus are gap junction events (not shown in Fig. 2 *A*, but see Fig. 6 *B*). Presumably, they reflect failed attempts of a new channel to open. This phenomenon was seen preferentially in cases of a large V_j. During the time period between physical membrane contact and first channel opening, there was no change in holding current attributable to a leak between the intra- and extracellular space. This suggests that formation of a gap junction channel is a tight process, i.e., the docking of two connexons must be complete *before* the new gap junction channel begins to conduct.

Conductance of single gap junction channels

According to Fig. 1 *A*, each preparation passed through a phase with only one operational gap junction channel. Using this phenomenon, we examined the influence of V_j on the conductance of a fully open channel, γ_j(*main state*). The following procedure was adopted to vary V_j systematically. In each experiment, before establishing a cell-to-cell contact, the membrane potentials of both cells were clamped to different voltages ($V_1 \neq V_2$). Specifically, V_2 was clamped to -100 to -75 mV, and V_1 was adjusted to give a V_j of 5–70 mV. The I_1 signals in Fig. 2 *A* were obtained in this way. Each trace shows the appearance of first channel currents. A comparison of the I_1 signals reveals that the amplitude of the open channel current grew with increasing V_j. Another feature was that, after the first slow opening, the channel always spent some time in its fully open state, irrespective of the amplitude V_j. Only thereafter was the channel ready for fast flickering.

Fig. 3 summarizes the results from 61 preparations. The conductance γ_j(*main state*) was plotted versus V_j. In each experiment, a single value of γ_j(*main state*) was obtained from the first channel opening. For this purpose, I_j was determined as the difference between the saturation current level and the zero current level. The graph shows that there is no significant correlation between γ_j(*main state*) and V_j ($r = 0.13$; $2\alpha > 0.1$). On average, the conductance of a fully open channel was 375 ± 6 pS ($n = 61$). This suggests that C6/36 cells possess a single type of gap junction channel whose maximal conductance is insensitive to V_j.

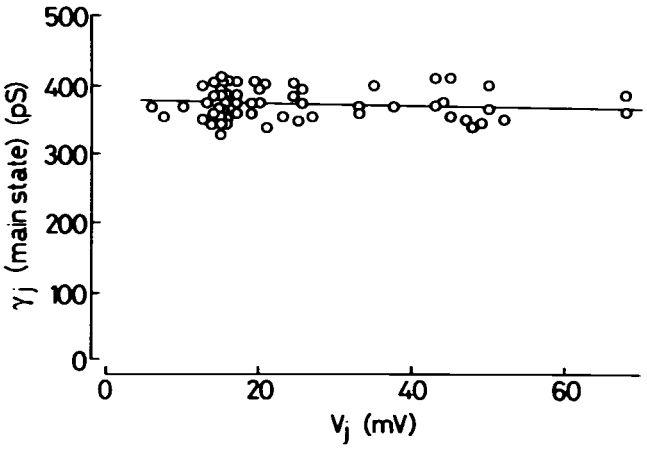

FIGURE 3 Relationship between the conductance of a fully open channel, γ_j(*main state*), and the transjunctional voltage gradient, V_j. Values of γ_j(*main state*) were obtained from first channel openings; each symbol represents another cell pair. Solid line: linear regression of γ_j(*main state*) versus V_j. There was no significant correlation between γ_j(*main state*) and V_j ($2\alpha > 0.1$; regression coefficient $r = 0.13$). The mean γ_j(*main state*) was 375 ± 6 pS ($n = 61$).

Gap junction channels exhibit a residual conductance

Fig. 4 shows an example of sequential formation of gap junction channels on an expanded time scale. In this case, V_1 and V_2 were clamped to -60 mV and -75 mV, respectively. Hence, V_j was -15 mV. Traces I_1 and I_2 show the associated currents of cells 1 and 2, respectively. At $t = 0$ s, the first channel began to operate. After 3.5 s, a second channel was apparent. Hence, between $t = 0$ s and 3.5 s, the synchronous current transitions are attributable to random openings (I_1, upward deflections; I_2, downward deflections) and closings of the same channel. During this period, I_1 and I_2 fluctuated between two discrete levels corresponding to the fully open channel (continuous line) and partially open channel (interrupted line). That is, I_1 and I_2 never returned to the level prevailing before channel opening. The current flow through the fully and partially open channels yielded conductances of 375 pS and 70 pS attributable to γ_j(*main state*) and γ_j(*residual*), respectively.

The current deflections after $t = 3.5$ s arise from the random operation of two channels in parallel. Given the channel properties described above, this should lead to three discrete current levels corresponding to 1) two fully open channels, 2) a fully open channel plus a partially open channel, and 3) two partially open channels. Examination of I_1 and I_2 indicates that this was the case. The large current level corresponds approximately to $2 \cdot \gamma_j$(*main state*), the middle level to γ_j(*main state*) + γ_j(*residual*), and the low level to $2 \cdot \gamma_j$(*residual*). This means that the second operational channel also failed to close completely. Residual conductances were not only present in this particular preparation, but were also seen in others (see, e.g., Figs. 1 *A* and 2). Common to all these cases is that, associated with fast channel transitions, I_1 (and I_2) never returned to 0, thus indicating incomplete channel closure.

Next, we explored whether or not γ_j(*residual*) depends on V_j. In each preparation examined, I_j exhibited distinct current levels attributable to γ_j(*residual*). To perform a quantitative analysis, a value of γ_j(*residual*) was gained from each experiment immediately after first channel formation. The residual current was determined as the difference between the lowest discrete current level and the zero coupling current. Fig. 5 shows the result of the analysis plotting γ_j(*residual*) versus V_j. Over the voltage range studied, i.e., $V_j = 9$–68 mV, γ_j(*residual*) decreased with increasing V_j. Linear regression

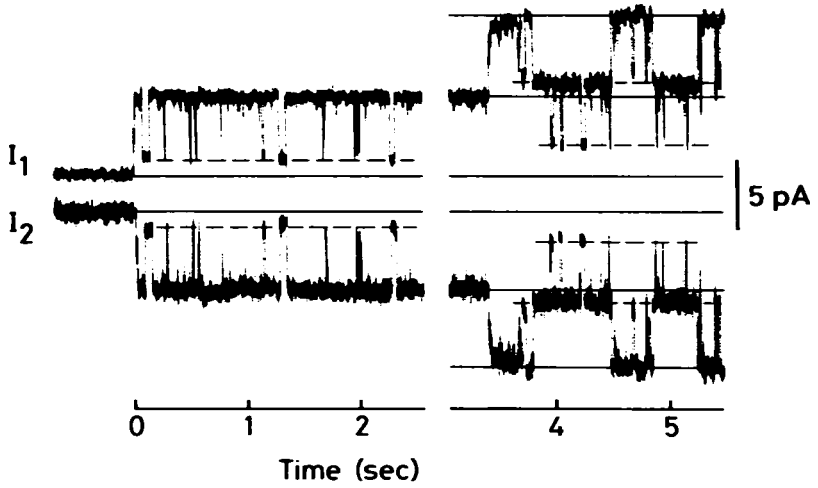

FIGURE 4 Sequential formation of gap junction channels reveals a residual conductance, $\gamma_j(residual)$. The membrane potentials of cells 1 and 2 (V_1 and V_2; not shown) were clamped to −60 mV and −75 mV, respectively. The associated membrane currents were measured continuously from both cells (I_1, I_2). Newly formed channels fluctuated between the fully open state (solid lines) and the residual state (dashed lines). t = 0 s corresponds to the first channel opening. Note the records are interrupted after 2.6 s.

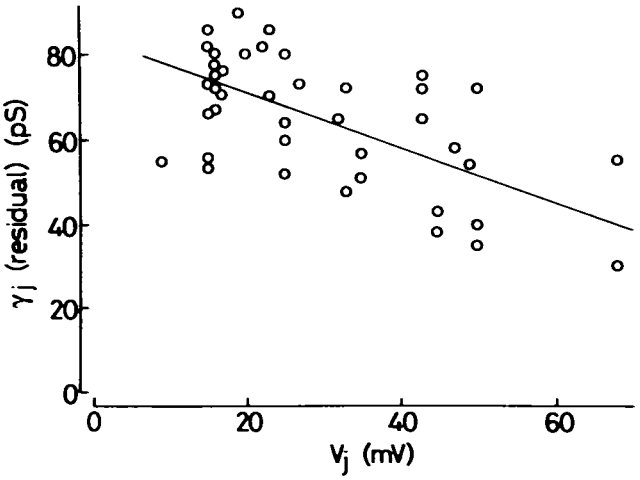

FIGURE 5 Dependence of the residual conductance, $\gamma_j(residual)$, on V_j. Each symbol corresponds to a single measurement obtained from a different preparation. Solid line: linear regression $\gamma_j(residual)$ versus V_j. There was a significant correlation between $\gamma_j(residual)$ and V_j ($2\alpha < 0.001$; correlation coefficient r = 0.62; n = 42) exhibiting a slope of −0.7 pS/mV.

analysis revealed a slope of −0.7 pS/mV, indicating a negative correlation between $\gamma_j(residual)$ and V_j (r = 0.62; $2\alpha <$ 0.001; n = 42). Extrapolation of V_j to 0 mV would lead to a $\gamma_j(residual)$ of 84 pS. Individual values of $\gamma_j(residual)$ ranged from 30 to 90 pS.

Gap junction channels show subconductance states

Fig. 6 shows two pairs of current records obtained under conditions similar to those in Figs. 1 *A* and 4. This means that before pushing the cells together, V_1 and V_2 were set to different levels. In this case, a large V_j was then established by clamping V_2 to −75 mV and V_1 to −30 mV (upper panel, V_j = −45 mV) or −10 mV (lower panel, V_j = −65 mV). In both cases, immediately after the first channel opening, I_j reached a maximum amplitude for a short period of time, corresponding to a $\gamma_j(main\ state)$ of 380 pS and 345 pS, respectively (presumably, the variability is related to the difference in temperature: Fig. 6 *A*, 26°C; Fig. 6 *B*, 22°C). Thereafter, I_j declined to lower levels, different from zero

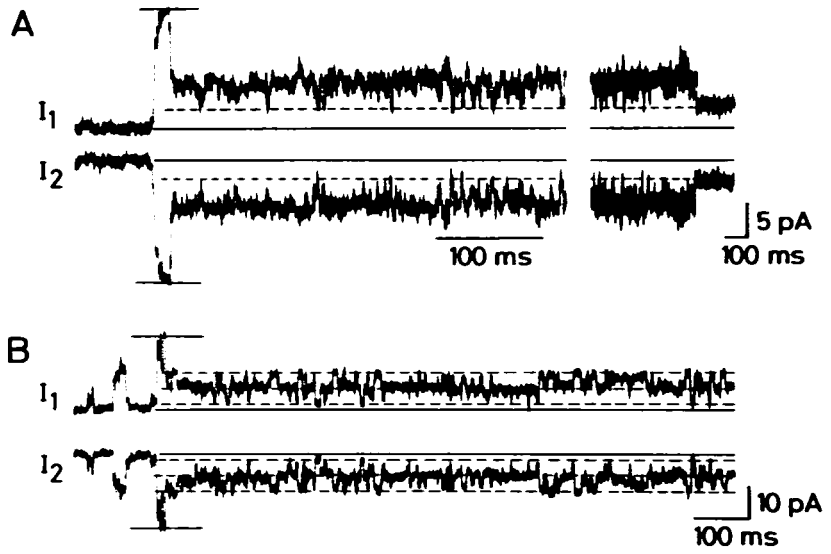

FIGURE 6 Existence of subconductance states, $\gamma_j(substate)$. At large V_j (*A*: V_j = −45 mV, i.e., V_1 = −30 mV and V_2 = −75 mV; *B*: V_j = −65 mV, i.e., V_1 = −10 mV and V_2 = −75 mV), a newly inserted channel remained only briefly in the fully open state. Thereafter, it started to flicker between the residual state and one substate (*A*) or two substates (*B*), respectively. Notice that in (*B*), the first and second trials did not lead to successful channel formation.

coupling current and in addition to the residual current level. As only one channel was present, all simultaneous transitions in I_1 and I_2 arose from openings and closings of the same channel. Hence, the extra current levels reflect the existence of subconductance states, γ_j(*substate*). In Fig. 6 *A*, despite the large noise, one additional current level is discernible. Toward the end of the traces, at compressed time resolution, the distinct current levels are more clearly visible, especially when I_j settled more permanently at the residual level. In Fig. 6 *B*, two additional substates are detectable. In this case, I_j fluctuated between three stable levels corresponding to the residual state and two substates. Examination of the discrete current steps in Fig. 6 revealed a γ_j(*substate*) of ~80 pS (Fig. 6 *A*) and ~60 pS (Fig. 6 *B*). The analysis of other experiments yielded similar results. On average, the current steps between substates corresponded to ⅓–¼ γ_j(*main state*).

In some experiments, we observed that the subconductance steps were not equally spaced between γ_j(*residual*) and γ_j(*main state*). The steps close to γ_j(*residual*) appeared to be larger than those close to γ_j(*main state*). This unexpected finding needs further investigation. However, it turned out that the substates are rather difficult to examine. Under steady-state conditions, substates were preferentially detectable over a limited range of V_j gradients, i.e., approximately 25 mV < V_j < 75 mV. In addition, upon application of V_j steps, the incidence of substate events declined as a function of time. Furthermore, substate activity was associated with an increase in I_j noise (see Fig. 6 *A*).

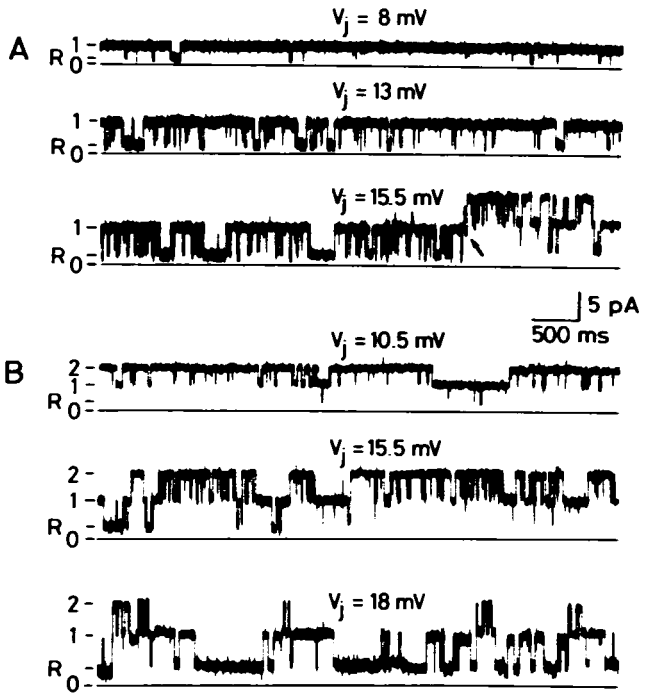

FIGURE 7 Dependence of single channel activity on V_j. (*A*) Cell pair with one channel. When V_j was increased from 8 mV (top) to 13 mV (center) and 15.5 mV (bottom), the channel spent progressively less time in the fully open state and more time in the residual state. Toward the end of the bottom trace, a second channel was inserted (see *arrow*). (*B*) Cell pair with two channels. When V_j was increased from 10.5 mV (top) to 15.5 mV (center) and 18 mV (bottom), both channels showed a decrease in dwell time in the fully open state. The records in (*A*) and (*B*) were taken in sequence. V_1 = −65 mV; V_2 was changed from −73 to −83 mV using 2.5-mV steps.

Dependence of single channel activity on V_j

In another series of experiments, the effect of V_j on single channel activity was further explored. For this purpose, we used newly formed cell pairs with one or two gap junction channels. The voltage-clamp protocol involved stepwise changes in V_j using increments of 2.5 mV. Fig. 7 *A* shows the case of a cell pair with one channel. The sequence of current records was obtained at V_j = 8 mV (top), 13 mV (center), and 15.5 mV (bottom). In each record, the channel exhibited fast transitions between γ_j(*main state*) and γ_j(*residual*). After the appearance of a second channel (see arrow in bottom trace), the minimal conductance increased to 2 · γ_j(*residual*), in agreement with Fig. 4 (see also the section Gap Junction Channels Exhibit a Residual Conductance, above). The analysis yielded a γ_j(*main state*) of 380 pS for the three traces.

More interestingly, however, a comparison of the current traces in Fig. 7 *A* suggests a correlation between the channel kinetics and V_j. The channel spent increasingly less time in the fully open state, *t*(*main state*), and more time in the residual state, when V_j was increased. Examination of the three records yielded the following values for the ratio *t*(*main state*)/*record duration*: 0.95, 0.85, and 0.7, respectively. These results suggest an inverse relationship between *t*(*main state*)/*record duration* and V_j. Fig. 7 *B*, a continuation of the current traces shown in Fig. 7 *A*, illustrates a case with two channels. The records were obtained at V_j = 10.5 mV (top), 15.5 mV (center), and 18 mV (bottom). The inverse relationship between *t*(*main state*)/*record duration* and V_j is also apparent under these conditions. When V_j was increased (top to bottom), I_j spent progressively less time at the level 2 · (I_j(*residual*) + I_j(*main state*)), and more time at 2 · I_j(*residual*).

When V_j was increased above 20 mV, the current signals grew more complex. The channel activity and hence the ratio *t*(*main state*)/*record duration* further declined with respect to time (see, e.g., Fig. 2). In addition, the I_j signals now revealed substates with respect to amplitude (see the section Gap Junction Channels Show Subconductance States, above). Fast transitions bracketed discrete current levels attributable to γ_j(*main state*), γ_j(*residual*), *and* γ_j(*substates*). This phenomenon was further explored using cell pairs with a single channel. In these cases, V_1 and V_2 were first clamped to −60 mV. Thereafter, voltage pulses of 200 ms duration, variable amplitude, and either polarity were applied to cell 1 every second. The resulting I_2 records were analyzed for gap junction events. In this case, the amplitude of the fast transitions were determined from the difference between discrete current levels, and the respective conductances, γ_j, calculated. The values obtained in this way correspond to the quantity commonly accessible in experiments performed on cell pairs whose gap junctions contain many channels (see, e.g., Burt and Spray, 1988; Rüdisüli and Weingart, 1989).

Fig. 8 summarizes the data from a single experiment of this kind. For each V_j examined, the values of γ_j were pooled in 16⅔ pS bins and plotted as frequency histograms. At the smallest voltage investigated, $V_j = \pm 25$ mV, the histograms revealed a binomial distribution (Fig. 8, *A* and *B*). The mean γ_j was estimated as 265 ± 5 pS ($n = 56$; range, 230–300 pS) for $V_j = +25$ mV, and 270 ± 4 pS ($n = 145$; range: 220–320 pS) for $V_j = -25$ mV. Application of a V_j of ± 50 mV (Fig. 8, *C* and *D*) gave rise to a different picture. The additional appearance of smaller I_j transitions drastically increased the range of γ_j values ($V_j = +50$ mV: 40–335 pS; $V_j = -50$ mV: 40–300 pS). As a consequence, the binomial distribution of γ_j was virtually lost. When V_j was increased to ± 75 mV (Fig. 8, *E* and *F*) this trend continued, leading to a further broadening of the data set ($V_j = +75$ mV, 40–340 pS; $V_j = -75$ mV, 40–315 pS). At $V_j = +100$ mV (Fig. 8 *G*; the preparation did not tolerate $V_j = -100$ mV), the histogram again looked different. Under these conditions, the large I_j transitions were missing. This gave rise to a narrow range of γ_j values (50–180 pS) and a binomial distribution again (mean $\gamma_j = 95 \pm 5$ pS; $n = 123$). Five additional experiments of this kind yielded similar results.

At first glance, the histograms in Fig. 8 suggest that γ_j is V_j-dependent. However, this conclusion is erroneous, because each histogram represents a different set of channel events. At small V_j (25 mV), γ_j corresponds primarily to the difference (1) between γ_j(*main state*) and γ_j(*residual*). At large V_j (100 mV), γ_j reflects mainly the steps (2) between individual substates. At intermediate V_j (50 mV, 75 mV), γ_j corresponds to a combination of (1) and (2). Pooling the data from the different histograms in Fig. 8 would lead to a multipeak distribution. Such histograms have been described for preformed cell pairs containing many gap junction channels (see, e.g., Rook et al., 1988; Kolb and Somogyi, 1991; Giaume et al., 1989; Chen and DeHaan, 1992). Our experiments performed on induced cell pairs with only one gap junction channel suggest that such histograms may result from channels exhibiting several conductance states rather than from gap junctions containing different types of channels.

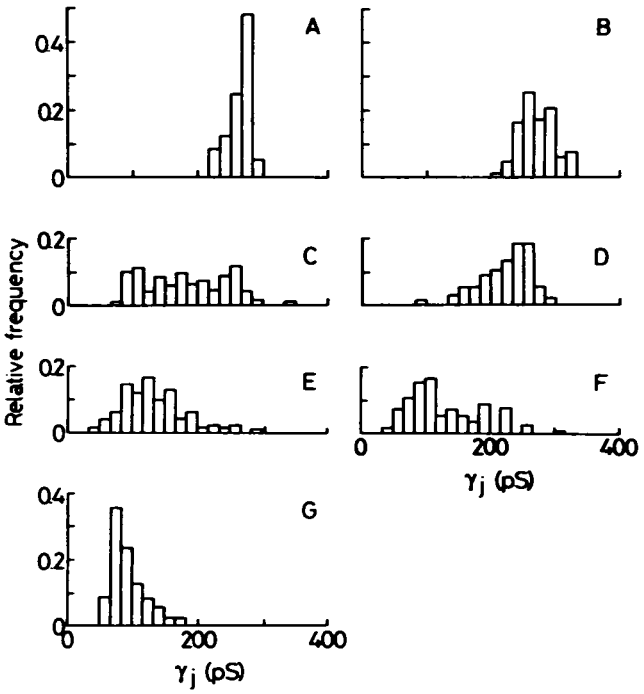

FIGURE 8 Frequency histograms of γ_j obtained at different transjunctional voltage gradients, V_j. Values of γ_j were gained from the analysis of the amplitude of discrete I_j transitions. Histograms associated with a V_j of ±25 mV (*A* and *B*) or +100 mV (*G*) revealed narrow distributions. Histograms related to a V_j of ±50 mV (*C* and *D*) or ±75 mV (*E* and *F*) yielded wide distributions. Individual values of γ_j were pooled in 16⅔-pS bins and plotted as relative frequencies.

Dependence of single channel activity on V_m

Some cell pairs persisted with a single gap junction channel for long periods of time (up to 3 min). They allowed us to explore the effects of the membrane potential, V_m, on channel activity. In these experiments, $V_{m,1}$ and $V_{m,2}$ were initially clamped to −60 mV and −75 mV. After channel formation, both cells were depolarized synchronously, i.e., identical voltage steps were administered to both cells, thus maintaining a constant V_j of −15 mV. Fig. 9 shows a representative series of paired records (I_1, I_2) obtained from the same experiment. They indicate that V_m did not affect γ_j(*main state*) or γ_j(*residual*), but modified the channel kinetics and the mode of channel activity. When $V_{m,1}$ was at −60 mV (Fig. 9 *A*), the channel fluctuated between two states, γ_j(*main state*) and γ_j(*residual*). In this record the ratio *t(main state)/record duration* was ~0.4. Depolarization of $V_{m,1}$ to −35 mV (Fig. 9 *B*) revealed no significant alterations, i.e., γ_j(*main state*) and γ_j(*residual*) were detectable, and *t(main state)/record duration* was ~0.6. When $V_{m,1}$ was depolarized to −10 mV (Fig. 9 *C*), there was a pronounced decrease in *t(main state)/record duration* to ~0.2. Surprisingly, when $V_{m,1}$ was depolarized to 15 mV (Fig. 9 *D*), the channel switched to a different mode. After a short period with fast transitions between γ_j(*main state*) and γ_j(*residual*) (*t(main state)/record duration* ~0.15), the channel underwent a slow transition between γ_j(*residual*) (dotted line) and its fully closed state, γ_j(*closed*). Later on, channel activity resumed after a slow transition between γ_j(*closed*) and γ_j(*residual*) (data not shown). When $V_{m,1}$ was depolarized to 60 mV (Fig. 9 *E*), I_j was reduced to 0, i.e., the channel remained in its closed state throughout.

Repolarization of $V_{m,1}$ and $V_{m,2}$ to −60 and −75 mV, respectively, restored the channel activity. The recovery pattern was dependent on both V_m and V_j. For example, the larger the previous depolarization of V_m, the slower was the recovery. As another example, a small V_j during recovery was associated with a transition between γ_j(*closed*) and γ_j(*residual*), whereas a large V_j was accompanied by a transition between γ_j(*closed*) and any other conducting state, i.e., γ_j(*residual*), γ_j(*substates*), or γ_j(*main state*). In all these cases, the reopenings always exhibited a slow time course. Furthermore, fast channel transitions only resumed after a slow channel opening.

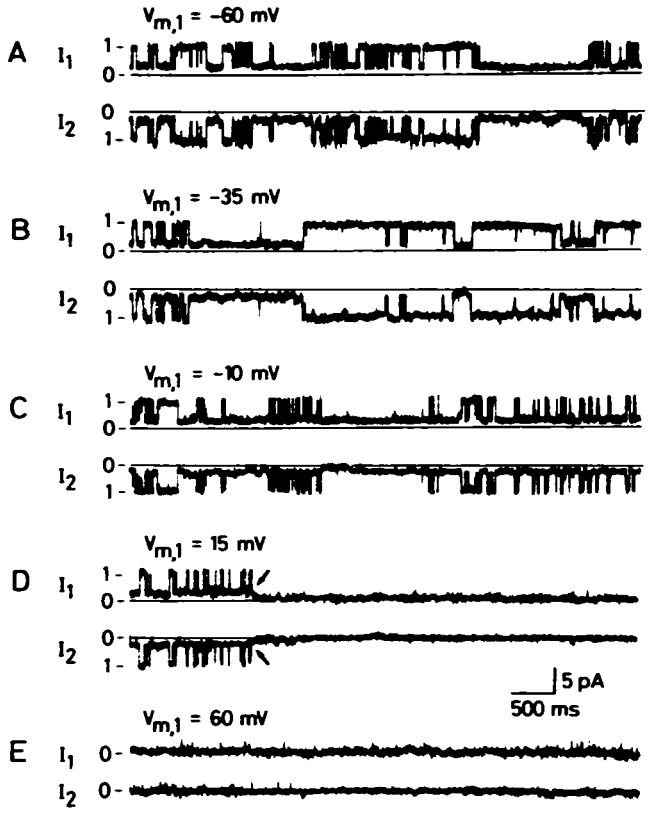

FIGURE 9 Dependence of single channel activity on membrane potential, V_m. V_j was maintained at −15 mV, whereas the membrane potential of both cells ($V_{m,1}$ and $V_{m,2}$) was depolarized synchronously and stepwise. Depolarization of $V_{m,1}$ from −60 mV (*A*) to −35 mV (*B*) and −10 mV (*C*) did not affect γ_j(*residual*) and γ_j(*main state*) but led to a decrease of the ratio *t(main state)/record duration* ($V_{m,1}$ = −60 mV: ~0.4 (*A*); $V_{m,1}$ = −35 mV: ~0.6 (*B*); $V_{m,1}$ = −10 mV: 0.2 (*C*)). At $V_{m,1}$ = 15 mV (*D*), the channel showed fast transitions involving γ_j(*main state*) and γ_j(*residual*). Suddenly it began a slow transition from γ_j(*residual*) to γ_j(*closed*) (see *arrows*) and remained silent. At $V_{m,1}$ = 60 mV (*E*), the channel was silent throughout.

Fast and slow channel transitions

According to Fig. 9, gap junction channels operate in two different modes, one involving fast current transitions, the other slow transitions. Fast transitions are complete within <2 ms (see, e.g., Fig. 2). They correspond to the transitions usually seen in membrane channels. Slow transitions last 20 to 70 times longer (see Fig. 9 *B*). They appear unique for insect gap junctions and hence require further examination.

Fig. 10 illustrates two examples of slow transitions at expanded time scale. In both cases, a sustained V_j gradient was maintained. Fig. 10 *A* shows a slow transition between γ_j(*main state*) and γ_j(*closed*). V_1 was clamped to −60 mV, V_2 to −75 mV. After few fast transitions involving γ_j(*main state*) and γ_j(*residual*), the channel exhibited a slow transition between γ_j(*main state*) and γ_j(*closed*), which lasted ~60 ms. Subsequently, there were no fast transitions starting from γ_j(*closed*). Such slow transitions did not only occur between γ_j(*closed*) and γ_j(*main state*). Fig. 10 *B* shows an example involving γ_j(*closed*) and γ_j(*residual*). V_1 was held at −61 mV, V_2 at −75 mV. Initially, the channel was closed completely and fast transitions were absent. Thereafter, the channel altered its state from γ_j(*closed*) to γ_j(*residual*) giving rise to a slow transition of ~20 ms duration. As a result, fast transitions started involving γ_j(*residual*) and γ_j(*main state*). Later, a slow transition of ~15 ms duration returned the channel from γ_j(*residual*) to γ_j(*closed*), thus terminating the fast channel activity.

The incidence of slow transitions was correlated with V_m. The frequency of occurrence increased with increasing depolarization. Below −40 mV, it was virtually zero. However, over the range of V_m that controls the macroscopic I_j, i.e., −10 mV to +30 mV (see Bukauskas et al., 1992), slow transitions between γ_j(*residual*) and γ_j(*closed*) were consistently observed. This suggests that V_m-dependent uncoupling may involve slow transitions.

Interaction between voltage sensitive gates

A gap junction channel consists of two identical hemichannels or connexons. Thus, it is assumed that each connexon possesses a V_j-sensitive gate, presumably located inside the conducting core. This raises the question whether or not both gates of a channel act simultaneously. To clarify this question, the following pulse protocol was adopted (Fig. 11 *A*; see also Harris et al., 1981). Initially, V_1 and V_2 were set to −40

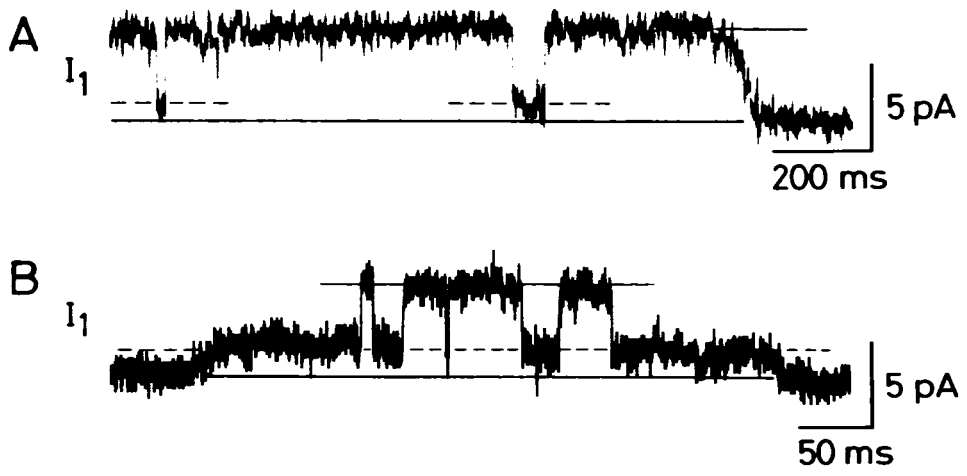

FIGURE 10 Fast versus slow channel transitions. (*A*) Fast transitions involving γ_j(*main state*) and γ_j(*residual*) are terminated by a slow transition from γ_j(*main state*) to γ_j(*closed*). V_1 = −60 mV, V_2 = −75 mV (not shown). (*B*) A slow transition between γ_j(*closed*) and γ_j(*residual*) turns on fast channel activity; a slow transition between γ_j(*residual*) and γ_j(*closed*) turns off fast channel activity. V_1 = −61 mV, V_2 = −75 mV (not shown).

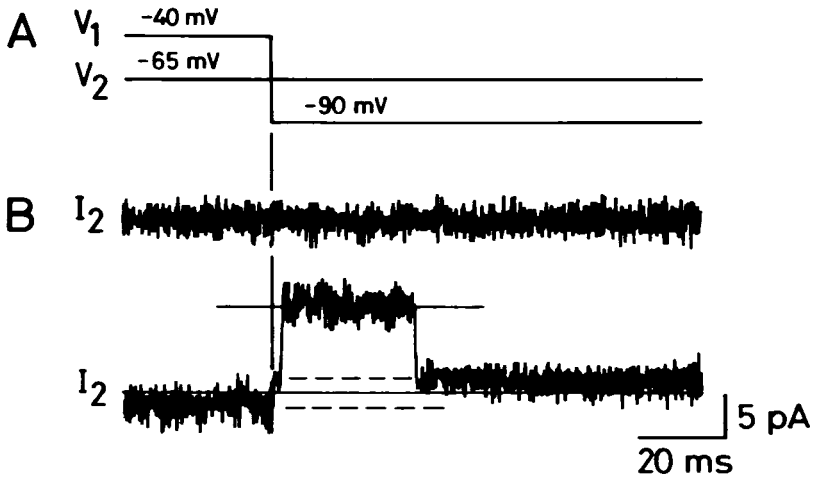

FIGURE 11 Interaction between the two V_j gates of a gap junction channel. (*A*) Pulse protocol used to produce a change in V_j polarity. (*B*) Selected current traces documenting the current flow across a gap junction channel. Top trace: Before changing the V_j polarity, the channel was in the closed state, $\gamma_j(closed)$. Bottom trace: Before V_j inversion, the channel was in the residual state, $\gamma_j(residual)$.

mV and −65 mV, establishing a V_j of −25 mV (inside of cell 1 positive with respect to cell 2). Suddenly, V_1 was changed to −90 mV, maintaining the amplitude of V_j but inverting its polarity (inside of cell 1 negative with respect to cell 2).

Fig. 11 *B* shows two selected I_2 records obtained in this way. In the first example, the channel was in the closed state for ~3 s because the fast channel activity was terminated by a slow transition from $\gamma_j(residual)$ to $\gamma_j(closed)$ (not shown). Switching the polarity of V_j did not restore channel activity. In the second example, at the beginning of the record the channel was in the residual state. Fast flickering had ceased shortly before (not shown). Inverting the polarity of V_j immediately yielded a residual current in the opposite direction, indicating that the channel maintained its conductive state, i.e., $\gamma_j(residual)$. After a short delay, the channel underwent a fast transition to its fully open state. Thereafter, it exhibited fast transitions between $\gamma_j(main\ state)$ and $\gamma_j(residual)$, and eventually settled on the latter. This behavior suggests that the change in V_j polarity readily opened a previously closed V_j gate. As a consequence, the V_j gradient became effective across the channel. The other V_j gate, which was previously open, now sensed V_j and responded by giving rise to fast flickering. The analysis of 20 experiments revealed that the time required for reopening a V_j gate was 2–10 ms. This interpretation of the single channel data is consistent with the results obtained from preformed pairs of C6/36 cells (Bukauskas and Weingart, unpublished observations) and amphibian blastomeres (Harris et al., 1981).

DISCUSSION

Formation of gap junctions can be induced by forcing two single cells into physical contact. In the past, this approach has been adapted to *Xenopus* blastulae (Loewenstein et al., 1978), *Xenopus* myoballs (Chow and Poo, 1984; Chow and Young, 1987) and rat cardiocytes (Rook et al., 1988). Here, we show that it is also applicable to the insect cell line C6/36. In conjunction with patch-pipettes and dual voltage-clamping, we were then able to study the formation of gap junction channels and examine their biophysical properties.

Formation of gap junction channels

It has been proposed that cell membranes contain precursors of gap junctions, so-called hemichannels or connexons (see, e.g., Bennett et al., 1991). Recently, evidence for this notion was gained from functional (DeVries and Schwartz, 1992) and topographical studies (Rahman et al., 1993). This raises the possibility that formation of a gap junction channel involves docking of two connexons located in adjacent cell membranes. Our experiments on C6/36 cells support this view. We found signs of intercellular coupling shortly after physical contact between two cells (~5 min). This suggests that a sizable number of connexons are present in the cell membranes, which undergo lateral diffusion. During gap junction formation, g_j increased in a sigmoid manner (Fig. 1 *C*). This observation suggests that channel formation is a cooperative process as previously proposed (Abney et al., 1987; Swenson et al., 1989). The formation of gap junctions reached a steady-state after ~20 min. This state may reflect an equilibrium between the rates of channel formation and degradation. However, cessation of channel insertion caused by a negative feedback mechanism cannot be ruled out. The conductance reached under steady-state conditions, g_j = 8.7 nS, corresponds to 23 channels (assuming a channel conductance of 375 pS; see the section Single Channel Conductances, below). For comparison, g_j in preformed pairs of C6/36 cells was 5–6 nS (Bukauskas et al., 1992). The data presented in Fig. 1 *C* allow an estimate of the rate of channel formation. The analysis involves the maximal slope, $\Delta g_j/\Delta t$, of the relationship g_j versus t: $\Delta n/\Delta t = \Delta g_j/\gamma_j \cdot \Delta t$, where γ_j = single channel conductance, and n = number of channels. Using this expression, $\Delta n/\Delta t$ turned out to be 2.5 channels/min. This is much lower than the value reported for insect hemocytes (60 channels/min; Churchill et al., 1993).

The molecular mechanisms involved in channel formation are largely unknown. Conceivably, the initial steps involve recognition of extracellular sites and anchorage via adhesion molecules (Keane et al., 1988; Meyer et al., 1992). Presumably, the subsequent steps include alignment of connexons, docking of two apposed connexons and opening of a

functional gap junction channel. The nature of the forces responsible for the integrity of gap junction channels are also obscure. Currently, it is debated whether covalent bonds are required to keep together the connexins and connexons of a channel (Dahl et al., 1991; Rahman et al., 1993). Our experiments give a few hints in this context. For example, during the formation of a gap junction channel, there was no leak between the intra- and extracellular space. This indicates that the assembly of two connexons is complete before the new channel begins to operate. Or, channel formation is an irreversible process. Gentle separation of two cells did not lead to a channel loss, indicating that the forces between the connexons and/or adhesion molecules are substantial. Also, on a few occasions we observed that I_j returned to 0 before the channel had reached its fully open state (see Figs. 2 *A* and 6 *B*). Presumably, this reflects a failure in channel opening rather than connexon docking.

A comparison of the properties of connexons and gap junction channels may further elucidate the process of channel formation. Conceivably, the properties of the connexons are preserved during the formation of a gap junction channel. However, it is also possible that the docking of two connexons modifies existing properties or introduces new ones. It turns out that this notion is not easy to pursue because of the scarcity of the available data. Currently, the electrical properties of connexons are known for horizontal cells of the catfish retina (DeVries and Schwartz, 1992). In these cells, the connexons have a V_m gate that undergoes fast transitions between an open and closed state. Under physiological conditions, they are closed because of a large $[Ca^{2+}]_i$ and the presence of a V_m. In most vertebrate cells, presumably also in horizontal cells, gap junction channels have a V_j gate that leads to partial uncoupling at large V_j. Obviously, this property is not easy to reconcile with the V_m gating seen in the connexons. In the case of the insect cell C6/36, a considerable amount of information is available concerning voltage gating (V_j and V_m gates) of gap junction channels (as in this article), but no data exist for connexons. Experiments on the latter will have to show if connexons and gap junction channels share some function properties.

Previously we have shown that C6/36 cells in culture can form intercellular cytoplasmic bridges (Bukauskas et al., 1993). This raises the question whether or not these cell-to-cell contacts result from physical contacts between cell membranes. However, this possibility can be ruled out by results obtained with induced cells pairs, e.g., the gating properties of I_j, or the response to heptanol (not shown).

Single channel conductances

The conductance of gap junction channels was determined in cell pairs with only one operational channel. We found that the channels exhibit several states with different conductances γ_j, a fully open state (γ_j(*main state*)), several substates (γ_j(*substates*)), a residual state (γ_j(*residual*)) and a closed state (γ_j(*closed*)).

γ_j(*main state*)

The conductance of a fully open channel was insensitive to V_j (voltage range examined: ±70 mV). The mean γ_j(*main state*), determined from first channel openings, turned out to be 375 pS. In previous studies carried out on preformed cell pairs, we reported a smaller and variable γ_j (100–250 pS; Bukauskas et al., 1992; Weingart et al., 1993). However, as explained in this paper (see the section Dependence of Single Channel Activity on V_j, and Fig. 8), because of interference from γ_j(*residual*) and γ_j(*substates*), the earlier estimates do not correspond to γ_j(*main state*). The value obtained from induced cell pairs, i.e., 375 pS, is in good agreement with an estimate derived from diffusion studies (400 pS; see Bukauskas et al., 1992) and close to that reported for induced pairs of insect hemocytes (325 pS; Churchill et al., 1993). It is larger than the values found for other arthropod preparations (epidermal insect cells, 288 pS, Churchill and Caveney, 1993; hepatopancreatic cells of crayfish, >200 pS, Chanson et al., 1994; lateral giant axon of earthworm, 100 pS, Brink and Fan, 1989). In our study, individual values of γ_j(*main state*) varied from 330 to 410 pS. Expressed as a percentage, this range is narrower than that usually seen in preformed pairs of mammalian cells after treatment with uncoupling agents (e.g., Burt and Spray, 1988; Rook et al., 1988; Rūdisūli and Weingart, 1989). This may reflect a large biological variability in case of mammalian gap junctions. However, our data on insect cells suggest another explanation: the channels of mammalian gap junctions may possess more than one conductance state, too. Hence, the broad γ_j histograms are likely to include transitions between substates (for illustration, see Fig. 8).

γ_j(*residual*)

Under quasiphysiological conditions ($V_m \sim -60$ mV; $V_j < 25$ mV), we observed fast I_j fluctuations between two stable levels corresponding to γ_j(*main state*) and γ_j(*residual*). The latter term emphasizes that the channel failed to close completely. Examination of first channel events revealed a mean γ_j(*residual*) of 65 pS, i.e., ~1/6 of γ_j(*main state*). Further analysis established a slight negative correlation between γ_j(*residual*) and V_j. This property may reflect gradual structural changes of the channel. Conceivably, the V_j subgates (see the section Operation of the Gap Junction Channel, below) align in a V_j-dependent manner and thereby affect the effective width of the pore. Alternatively, the presence of a small and large γ_j may indicate the coexistence of two channels of different unitary conductance. This explanation seems unlikely because we never observed formation of 65-pS channels. In addition, in cell pairs containing several gap junction channels, the number of residual steps always matched the number of channels inserted (for further arguments, see the section Fast Versus Slow Channel

Transitions, below). However, some authors reported γ_j data sets with a small and large conductance and attributed it to the presence of two types of channels (e.g., Rook et al., 1988).

The change from γ_j(*main state*) to γ_j(*residual*) may be brought about by different mechanisms: an electrostatic barrier, and a steric barrier. In the case of the electrostatic barrier, channel permeation may be limited by electrostatic interactions between the ions and the pore (discrimination by charge). With a steric barrier, permeation may be limited by the lumen of the pore (discrimination by size). However, the data currently available do not allow us to decide between these possibilities.

Previous studies on preformed pairs of C3/36 cells have shown that g_j does not decrease to 0 in the presence of a large V_j (Bukauskas et al., 1992). This property may be explained by incomplete channel closure, i.e., the existence of Vγ_j(*residual*). Partial decline in g_j at large V_j is a frequent finding in vertebrate gap junctions, too (for references, see Bennett and Verselis, 1992; for an exception, see Chanson et al., 1993). Therefore, it is possible that their channels also possess a γ_j(*residual*). Preliminary experiments with neonatal cardiac myocytes and transfected cells expressing Cx43 support this view. (K. Banach, F. F. Bukauskas, V. Valiunas and R. Weingart, unpublished observations). At present, we can only speculate about the biological significance of γ_j(*residual*). Conceivably, it provides a mechanism to modulate intercellular signaling, e.g., by switching from molecular to ionic coupling.

γ_j(substates)

At $V_j > \pm 25$ mV, we observed additional discrete current levels intermediate to γ_j(*main state*) and γ_j(*residual*); hence, they were named γ_j(*substates*). Their presence suggests that the mechanism of V_j-gating involves several subgates. The current steps between individual substates yielded conductances of 50–80 pS, corresponding to ⅓–¼ of γ_j(*main state*). However, a quantitative analysis of substate events turned out to be difficult for the following reasons. 1) Because of the inverse relationship between γ_j(*residual*) and V_j (see Fig. 5), the substates are expected to be proportional to V_j. 2) It appears that the substates are spaced unequally between γ_j(*main state*) and γ_j(*residual*). We observed a tendency for smaller steps toward the fully open state of the channels. 3) The occurrence of substates was associated with an increase in noise (see Fig. 6 *A*). 4) Substates were present over a particular V_j range and for a limited time only. They were virtually absent at ± 25 mV > V_j > ± 75 mV and late during V_j pulses. These aspects not only reflect the difficulties encountered when studying substate events, they also raise interesting questions related to the operation of V_j subgates. However, more experiments are needed to elucidate the underlying mechanisms.

The operation of γ_j(*substates*) offers an explanation for the bell-shaped relationship between V_j and g_j previously described for preformed pairs of C3/36 cells (Bukauskas et al., 1992). As V_j is increased beyond ± 25 mV, the preferential state of the channels gradually shifted from γ_j(*main state*) to γ_j(*substates*) and γ_j(*residual*). Recently, substates of gap junction channels have been observed in two other arthropod preparations, in epidermal cells of an insect (Churchill and Caveney, 1993) and in giant axons of the earthworm (Ramanan and Brink, 1993). However, because of the limited number of observations (former reference) and the variability in conductance (latter reference), it was not possible to determine unitary substeps. Preliminary experiments with induced pairs indicated the existence of substates in neonatal cardiac myocytes (F. F. Bukauskas and R. Weingart, unpublished observations). Previously, some investigators have postulated substates for gap junction channels of vertebrates (e.g., Rook et al., 1988; Kolb and Somogyi, 1991; Chen and DeHaan, 1992). However, using preformed cell pairs with multichannel gap junctions, these authors could not exclude an involvement of several channel populations or cooperativity between channels of a single population.

Fast versus slow channel transitions

The I_j signals revealed two types of transitions, fast transitions that were complete within <2 ms, and slow transitions which lasted 15–60 ms (see Fig. 10). The fast transitions occurred between current levels corresponding to γ_j(*main state*), γ_j(*substates*), and γ_j(*residual*), but never involved γ_j(*closed*). Therefore, γ_j(*residual*) may be regarded as baseline for fast channel activity. As already mentioned (see the section Single Channel Conductances, above), fast transitions controlled by V_j-sensitive gating are involved in the bell-shaped relationship between g_j and V_j. The slow transitions occurred between current levels corresponding to γ_j(*closed*) and any one of the following states, γ_j(*main state*), γ_j(*substates*) or γ_j(*residual*). Hence, γ_j(*closed*) may be viewed as baseline for slow channel activity. It turned out that the slow transitions are controlled by V_m-sensitive gating and hence determine the inverse S-shaped relationship between g_j and V_m previously found in preformed cell pairs (Bukauskas et al., 1992). In these preparations, g_j was large at negative V_m because the channels were mainly in the open state. Upon depolarization, g_j decreased and eventually declined to 0 because the channels undergo slow transitions to reach γ_j(*closed*) and hence stop fast flickering. Previous experiments on induced pairs of C6/36 cells suggested that γ_j may be sensitive to V_m (Weingart et al., 1993). Considering the data gained in this study from induced cell pairs, this interpretation is no longer tenable.

The fast transitions conform to the transitions usually observed in membrane channels, whereas the slow transitions are quite different. The latter resemble the process of first channel opening (see the section Formation of Gap Junction Channels, above). However, there is a major difference. During first channel opening, fast flickering never starts from γ_j(*residual*) but always from γ_j(*main state*). Interestingly, slow channel openings and closings have been seen in preformed pairs of rat lacrimal gland cells and guinea pig

cardiac myocytes (Neyton and Trautmann, 1985; Rūdisūli and Weingart, 1989). Experiments with induced cell pairs will show if they are related to the slow transitions observed in C6/36 cells.

Operation of the gap junction channel

Gap junction channels of C6/36 cells seem to have two types of voltage-sensitive gates, one controlled by transjunctional voltage (V_j gate), and the other by membrane potential (V_m gate). This conclusion is based on both macroscopic (Bukauskas et al., 1992) and microscopic I_j measurements (shown in this article). In an attempt to incorporate the functional data available, the following scheme emerges for the operation of an insect gap junction.

The V_j-dependent gating mechanism consists of several subgates. Their operation leads to fast I_j transitions involving γ_j(*main state*), γ_j(*substates*), and γ_j(*residual*), but not γ_j(*closed*). The subgates are all open at γ_j(*main state*) and all closed at γ_j(*residual*), whereas some are open and some closed at γ_j(*substates*). At V_j = 0 mV the channel is preferentially in the main state, at large V_j it resides mainly in the residual state, and at intermediate V_j it is in the main state, a substate, or the residual state. The recovery of V_j gate activity is fast (see Fig. 11). Reopening of closed V_j gates occurs within 2–10 ms. Comparable to V_j gating, presumably the V_m-dependent gating also possesses several subgates. However, so far it has been difficult to demonstrate substates. The operation of the V_m gate leads to slow I_j transitions. The slow transitions start from γ_j(*closed*) or terminate at γ_j(*closed*). That is, they occur between γ_j(*closed*) and any one of the following states: γ_j(*main state*), γ_j(*substates*), or γ_j(*residual*). The probability for the V_m gate to be open depends on V_m. At negative V_m the channel is open, i.e., V_j-dependent fast channel activity operates. Upon depolarization the channel undergoes slow transitions and closes completely, i.e., fast channel activity ceases.

A gap junction channel is built of two connexons and hence may accommodate two sets of V_j subgates presumably located inside the channel. At V_j = 0 mV the channel is open, i.e., the subgates are in the resting position. In this configuration, the channel is able to sense a voltage. Thus, application of a V_j gradient leads to the recruitment of one set of V_j subgates. V_j is sensed by the subgates exposed to the positive side of the voltage gradient (Bukauskas and Weingart, manuscript in preparation). Each gap junction channel possesses a V_m gate presumably located inside the channel close to the area of contact between the connexons.

In summary, in the past preformed cell pairs have been used extensively to explore the electrical properties of gap junction channels (see Bennett et al., 1991; Bennett and Verselis, 1992). However, it is obvious that the existence of multiple conductances renders it difficult to extract meaningful information about single channels from such preparations. As demonstrated in this paper, induced cell pairs offer a powerful alternative.

The authors are indebted to Dr. C. Kempf for providing the C6/36 cells; to Marlis Herrenschwand and Magda Spycher for technical assistance; and to Peter Clamann for help with the language.

This work was supported by the Swiss National Science Foundation (grants 31-25'333.88 and 31-36'046.92) and the Swiss Academy of Medical Sciences (F. F. B.).

REFERENCES

Abney, J. R., J. Braun, and J. C. Owicki. 1987. Lateral interactions among membrane proteins: implications for the organization of gap junctions. *Biophys. J.* 52:441–454.

Bennett, M. V. L., and V. K. Verselis. 1992. Biophysics of gap junctions. *Cell Biol.* 3:29–47.

Bennett, M. V. L., L. C. Barrio, T. A. Bargiello,, D. C. Spray, E. Hertzberg, and J. C. Saez. 1991. Gap junctions: new tools, new answers, new questions. *Neuron.* 6:305–320.

Brink, P. R., and S. Fan. 1989. Patch clamp recordings from membranes which contain gap junction channels. *Biophys. J.* 56:579–593.

Bukauskas, F., C. Kempf, and R. Weingart. 1992. Electrical coupling between cells of the insect *Aedes albopictus*. *J. Physiol. (Lond).* 448: 321–337.

Bukauskas, F. F., and R. Weingart. 1993. Multiple conductance states of newly formed single gap junction channels. *Pfluegers Arch. Eur. J. Physiol.* 423:152–154.

Bukauskas, F., C. Kempf, and R. Weingart. 1993. Cytoplasmic bridges and gap junctions in an insect cell line (*Aedes albopictus*). *J. Exp. Physiol.* 77:903–911.

Burt, J. M., and D. C. Spray. 1988. Single-channel events and gating behavior of the cardiac gap junction channel. *Proc. Natl. Acad. Sci. USA.* 85:3431–3434.

Chanson M., K. J. Chandross, M. B. Rook, J. A. Kessler, and D. C. Spray. 1993. Gating characteristics of a steeply voltage-dependent gap junction channel in rat Schwann cells. *J. Gen. Physiol.* 102:925–946.

Chanson M., C. Roy, and D. C. Spray. 1994. Voltage-dependent gap junctional conductance in hepatopancreatic cells of *Procambarus clarkii*. *Am. J. Physiol.* 266:C569-C577.

Chen Y., and R. L. DeHaan. 1992. Multiple-channel conductance states and voltage regulation of embryonic chick cardiac gap junctions. *J. Membr. Biol.* 127:95–111.

Chow, I., and M.-M. Poo. 1984. Formation of electrical coupling between embryonic *Xenopus* muscle cells in culture. *J. Physiol. (Lond).* 346: 181–194.

Chow, I., and S. H. Young. 1987. Opening of single gap junction channels during formation of electrical coupling between embryonic muscle cells. *Dev. Biol.* 122:332–337.

Churchill, D., and S. Caveney. 1993. Double whole-cell patch-clamp of gap junctions in insect epidermal cell pairs: single channel conductance, voltage dependence, and spontaneous uncoupling. *In* Gap Junctions: Progress in Cell Research, Vol. 3. J. E. Hall, G. A. Zampighi, and R. M. Davis, editors. Elsevier, Amsterdam. 239–245.

Churchill, D., S. Coodin, R. R. Shivers, and S. Caveney. 1993. Rapid *de novo* formation of gap junctions between insect hemocytes in vitro: a freeze-fracture, dye-transfer and patch-clamp study. *J. Cell Sci.* 104: 763–772.

Dahl, G., E. Levine, C. Rabadan-Diehl, and R. Werner. 1991. Cell/cell channel formation involves disulfide exchange. *Eur. J. Biochem.* 197: 141–144.

DeVries, S. H., and E. A. Schwartz. 1992. Hemi-gap junction channels in solitary horizontal cells of the catfish retina. *J. Physiol. (Lond).* 445: 201–230.

Igarashi, A. 1978. Isolation of a Singh's *Aedes albopictus* cell clone sensitive to Dengue and Chikungunya viruses. *J. Gen. Virol.* 40: 531–544.

Giaume, C., C. Randriamampita, and A. Trautmann. 1989. Arachidonic acid closes gap junction channels in rat lacrimal gland cells. *Pfluegers Arch. Eur. J. Physiol.* 413:273–279.

Harris, A. L., D. C. Spray, and M. V. L. Bennett. 1981. Kinetic properties of a voltage-dependent junctional conductance. *J. Gen. Physiol.* 77: 95–117.

Keane, R. W., P. P. Mehta, B. Rose, L. S. Honig, W. R. Loewenstein, and U. Rutishauser. 1988. Neural differentiation, NCAM-mediated adhesion, and gap junctional communication in neuroectoderm. A study in vitro. *J. Cell Biol.* 106:1307–1319.

Kolb, H.-A., and R. Somogyi. 1991. Characteristics of single channels of pancreatic acinar gap junctions subjected to different uncoupling procedures. *In* Biophysics of Gap Junctions. C. Peracchia, editor. CRC Press, Boca Raton. 209–228.

Loewenstein, W. R., Y. Kanno, and S. J. Socolar. 1978. Quantum jumps of conductance during formation of membrane channels at cell-cell junction. *Nature (Lond).* 274:133–136.

Meyer, R. A., D. W. Laird, J.-P. Revel, and R. G. Johnson. 1992. Inhibition of gap junction and adherens junction assembly by connexin and A-CAM antibodies. *J. Cell Biol.* 119:179–189.

Neyton, J., and A. Trautmann. 1985. Single channel currents of an intercellular junction. *Nature (Lond).* 377:283–295.

Rahman, S., G. Carlile, and W. H. Evans. 1993. Assembly of hepatic gap junctions. *J. Biol. Chem.* 268:1260–1265.

Ramanan, S. V., and P. Brink. 1993. Multichannel recordings from membranes which contain gap junctions. II. Substates and conductance shifts. *Biophys. J.* 65:1387–1395.

Rook, M. B., H. J. Jongsma, and A. C. G. van Ginneken. 1988. Properties of single gap junction channels between isolated neonatal rat heart cells. *Am. J. Physiol.* 255:H770–H782.

Rūdisūli, A., and R. Weingart. 1989. Electrical properties of gap junction channels in guinea-pig ventricular cell pairs revealed by exposure to heptanol. *Pfluegers Arch. Eur. J. Physiol.* 415:12–21.

Swenson, K. I., J. R. Jordan, E. C. Beyer, and D. L. Paul. 1989. Formation of gap junctions by expression of connexins in *Xenopus* oocytes pairs. *Cell* 57:145–155.

Verselis, V. K., M. V. L. Bennett, T. A. Bargiello. 1991. A voltage-dependent gap junction in *Drosophila melanogaster*. *Biophys. J.* 59:114–126.

Weingart, R. 1986. Electrical properties of the nexal membrane studied in rat ventricular cell pairs. *J. Physiol. (Lond).* 370:267–284.

Weingart, R., and F. F. Bukauskas. 1993. Gap junction channels of insect cells exhibit a residual conductance. *Pfluegers Arch. Eur. J. Physiol.* 424:192–194.

Weingart, R., F. F. Bukauskas, and C. Kempf. 1993. Insect cell pairs: electrical properties of intercellular junctions. *In* Gap Junctions: Progress in Cell Research, Vol. 3. J. E. Hall, G. A. Zampighi, and R. M. Davis, editors. Elsevier, Amsterdam. 247–252.